J. Environ. Radioactivity **24** (1994) 159–179

A Modelling Study of ^{226}Ra Dispersion in an Estuarine System in South-West Spain

R. Periáñez,[a] J. M. Abril[b] & M. García-León[a]

[a]Dpto. Física Atómica, Molecular y Nuclear, Universidad de Sevilla, Apdo. 1065, 41080-Sevilla, Spain

[b]Dpto. Física Aplicada, E. U. Ingeniería Técnica Agrícola, Universidad de Sevilla, Ctra. Utrera Km. 1, 41014-Sevilla, Spain

(Received 2 June 1993; revised version received 24 November 1993; accepted 1 December 1993)

ABSTRACT

A numerical model to study ^{226}Ra dispersion in the Odiel River, in which two fertilizer plants release their wastes, has been developed. The hydrodynamic equations have been solved to obtain the instantaneous water state which allows us to describe the advective and diffusive transport of the radionuclides. The hydrodynamic model has been calibrated in order to reproduce field data. Diffusion coefficients have been formulated taking into account the shear effect. Good agreement between calculated and experimentally measured ^{226}Ra concentrations has been achieved. The source term, which was unknown, has been investigated and found to be comparable to that of other fertilizer plants.

1 INTRODUCTION

The radiological impact in rivers due to releases from phosphate fertilizer plants is well established (Paul *et al.*, 1980; Kobal *et al.*, 1990; Koster *et al.*, 1991). Recently, it has been found (Periáñez & García-León, 1993) that anomalous ^{226}Ra activities were present in waters collected at the Odiel River (which is located in south-west Spain; see Fig. 1), where two

J. Environ. Radioactivity 0265-931X/94/$07·00

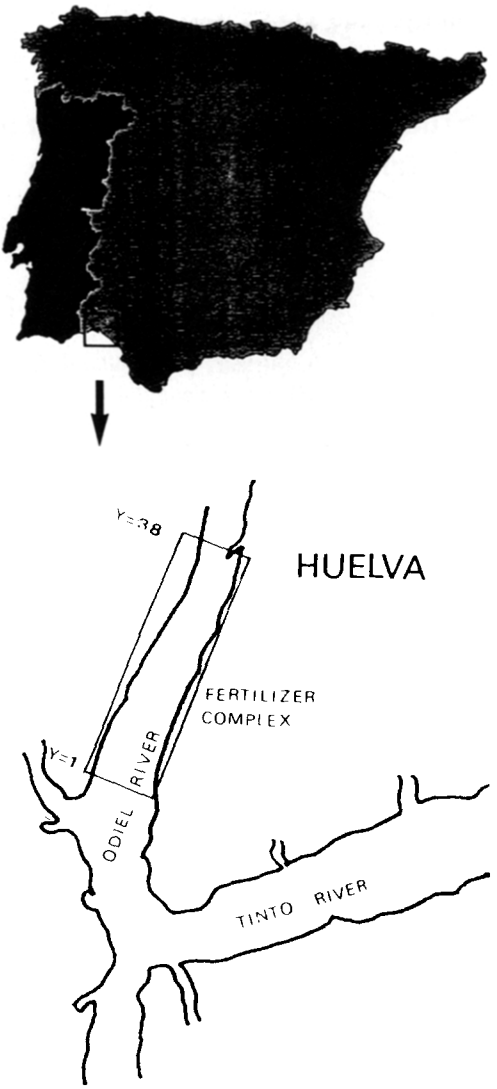

Fig. 1. Map of the Odiel River and its location in Spain. The rectangular box is the grid that has been used in the model.

fertilizer plants release their wastes. The zone under study is an estuarine system, so it is affected by tidal oscillations.

Two sampling campaigns were performed; one during July 1990 (dry season) and the other one during March 1991 (wet season). Two water samples were collected from each sampling station; one during high water and the other during low water. The experimental results obtained from this work allowed the authors to confirm the radiological impact of the fertilizer

complex in the river. Furthermore, they directed the authors to consider in more detail the influence of tidal oscillations and weather conditions on the activity concentrations in the river, as well as the magnitude of the activity input from the fertilizer complex, which is not known.

In this paper a numerical model is developed to simulate the tide and wind induced dispersion of a conservative substance in the Odiel river. This model has been applied to study ^{226}Ra dispersion in this environment and it has been shown to be able to reproduce the experimental data. Consequently, it could be used to predict the radiological impact in the river from a known amount of activity discharged in the water.

As mentioned before, ^{226}Ra is treated as a conservative substance. This assumption is realistic since in the estuarine system studied here, up to 90% (Periáñez *et al.*, 1994) of the ^{226}Ra activity per litre of water is in dissolved form. Thus, ionic exchanges between dissolved and suspended matter can be neglected as a first approach. This effect has also been found in other estuaries; for instance, in Winyah Bay estuary up to 80% of the ^{226}Ra activity is in dissolved form (Elsinger & Moore, 1980).

Two transport mechanisms must be considered to study radionuclide dispersion in an aquatic environment: diffusion and advection. The problem of dispersion is treated here by solving the hydrodynamic equations with appropriate choices for boundary conditions and other factors. The advection term is obtained from the velocity field that results from the hydrodynamic equations and the diffusion term is formulated to include the shear effect. This conceptual model is presented in Section 2.

In Section 3 a numerical model is presented. Based on a study of numerical dispersion and a stability condition, the authors have established the temporal and spatial scales for the model and defined a grid covering that part of the Odiel River under study. The boundary conditions used for the hydrodynamic and dispersion model are also defined.

The results are presented in Section 4. The source term is not known, so the authors have looked for one which produces the best agreement between observed and calculated ^{226}Ra concentrations. The inferred source term has been found to be comparable to those of other fertilizer plants, as given in current literature.

Finally, some sensitivity tests have been performed in order to study the model response to variations in diffusion coefficients, boundary conditions and source term magnitude. These are presented in Section 5.

2 CONCEPTUAL MODEL

The hydrodynamic equations for vertically averaged motion can be written as (Pugh, 1987):

$$\frac{\partial z}{\partial t} + \frac{\partial}{\partial x}[(D+z)u] + \frac{\partial}{\partial y}[(D+z)v] = 0 \tag{1}$$

$$\frac{\partial u}{\partial t} + v\frac{\partial u}{\partial y} + u\frac{\partial u}{\partial x} + g\frac{\partial z}{\partial x} - \Omega v + K\frac{u\sqrt{u^2+v^2}}{D+z} - \frac{\rho_a}{\rho_w}\frac{C_D}{D+z}|W|W\cos\theta = 0 \tag{2}$$

$$\frac{\partial u}{\partial t} + v\frac{\partial v}{\partial y} + u\frac{\partial v}{\partial x} + g\frac{\partial z}{\partial y} + \Omega u + K\frac{u\sqrt{u^2+v^2}}{D+z} - \frac{\rho_a}{\rho_w}\frac{C_D}{D+z}|W|W\mathrm{sen}\theta = 0 \tag{3}$$

where u and v are the depth averaged water velocities along the x and y axes respectively, D is the depth of water below the mean sea level and z is the displacement of the water level from the mean; g is the gravitational constant, Ω is the Coriolis parameter and K is the bed friction coefficient. The value of Ω is $\Omega = 2w\,\mathrm{sen}\,\lambda$, where w is the earth's rotational angular velocity and λ is the latitude. Typical values of K range from 0·0015 to 0·0025 (Pugh, 1987).

The last term is the response to wind stress: ρ_a and ρ_w are the air and water densities, W the wind velocity, θ the direction to which the wind blows measured anticlockwise from east and C_D is a dimensionless drag coefficient. An acceptable value for C_D (Pugh, 1987) is given by:

$$C_D = (0{\cdot}63 + 0{\cdot}066W)10^{-3}$$

for $2{\cdot}5 < W < 21$, with W measured in ms^{-1}, 10 m above the sea surface.

The response to atmospheric pressure has been included in the model. For a variation ΔP about the mean atmospheric pressure over the water, the mean sea level of water will change according to:

$$\Delta D = -\frac{\Delta P}{\rho_w g} \tag{4}$$

This response is called the inverted barometer effect (Pugh, 1987). We include neither spatial gradients in atmospheric pressure nor mobile atmospheric heads because of the small dimensions of our estuarine site (about 4 km length).

Once the hydrodynamic equations have been solved, the next step is to treat the problem of dispersion of a conservative substance. The advective–diffusion equation for an incompressible flow in two dimensions can be written as (Prandle, 1984):

$$\frac{\partial C}{\partial t} + u\frac{\partial C}{\partial x} + v\frac{\partial C}{\partial y} = \frac{1}{H}\left[\frac{\partial}{\partial x}\left(HK_u\frac{\partial C}{\partial x}\right) + \frac{\partial}{\partial y}\left(HK_v\frac{\partial C}{\partial y}\right)\right] \tag{5}$$

where C is the depth averaged concentration which depends on the instantaneous water level, $H = D + z$. Second and third terms represent advective transport and the last term represents diffusion. K_u and K_v are the diffusion coefficients along the x and y directions, respectively. In order to take into account the shear effect, the diffusion coefficients have been formulated as (Prandle, 1984):

$$\begin{aligned} K_u &= \beta_1 |u| \sqrt{u^2 + v^2} \\ K_v &= \beta_2 |v| \sqrt{u^2 + v^2} \end{aligned} \tag{6}$$

where β_1 and β_2 are numerical factors to be calibrated for each specific site.

3 THE NUMERICAL MODEL

A set of differential equations must be solved, so a spatial and temporal discretization of the site will be carried out.

The spatial and temporal resolution of the model will be selected so as to verify the Courant-Friederich-Lewy (C-F-L) criterion and to minimize numerical dispersion.

The first condition establishes that

$$\Delta t < \frac{\Delta x}{\sqrt{2gD_m}} \tag{7}$$

where D_m is the maximum water depth of the river.

However, the hypothesis of instantaneous and homogeneous mixing in each model compartment produces numerical dispersion. This effect is equivalent to the addition of an amount K' to the diffusion coefficient K (Prandle, 1984), where

$$K' = \frac{1}{2}(u\Delta x - u^2\Delta t) \tag{8}$$

The authors have chosen $\Delta t = 6$ s and $\Delta x = \Delta y = 100$ m. D_m is about 8 m for the studied estuarine site, so the C-F-L criterion is automatically satisfied.

As a first estimate, $\beta_1 = \beta_2 = 1000$ s are taken, which are the values found in current literature (Prandle, 1984). The magnitude of the velocities

u and v are known from field data (work done by the Puerto Autónomo de Huelva, 1989); so while levels are increasing and decreasing the absolute values of the velocities are $u \approx 0{\cdot}11\,\mathrm{ms}^{-1}$ and $v \approx 0{\cdot}56\,\mathrm{ms}^{-1}$. With the diffusion coefficients used, we obtain $K_u = 63$ and $K_v = 320\,\mathrm{m}^2\,\mathrm{s}^{-1}$. On the other hand, $K'_u = 5{\cdot}4$ and $K'_v = 27\,\mathrm{m}^2\,\mathrm{s}^{-1}$, so that K' is 8% of K. When $u = v = 0$ then $K_u = K_v = K'_u = K'_v = 0$, so there is no diffusive transport. Finally, if $v \approx 10^{-3}\,\mathrm{ms}^{-1}$ then $K_v = 10^{-3}$ and $K'_v = 0{\cdot}05\,\mathrm{m}^2\,\mathrm{s}^{-1}$. It is concluded that numerical dispersion is greater than diffusive transport only during a short time at high and low water, and that when it takes place, its absolute value is very close to zero. Diffusive transport is important only with high values for the velocities, but then numerical dispersion is less than the diffusion coefficients, so the diffusive transport can be calibrated.

The grid used in the model is shown in Fig. 2(a). It includes 456 cells, each cell containing either water or land. The depth was taken from marine charts and introduced as input data for each compartment.

A centred finite difference scheme was adopted to solve the hydrodynamic equations; the schematic representation is shown in Fig. 2(b). By centring the bed friction term, an improved convergence of the hydrodynamic model is achieved (Prandle, 1984).

Still-water initial conditions (Prandle, 1974) were used in initializing the model. This consists of taking $z = u = v = 0$ for $t = 0$. So, before discharging the contaminants, several tidal cycles must elapse in order to allow the model equations to reach a state in which the solutions of the equations represent the system under study (the estuarine site).

Water elevations were specified along the southern border for each time step. These elevations were obtained from the work performed by the Puerto autónomo de Huelva (1989). The hydrodynamic model calibration has been carried out with hydraulic and meteorological data from 4 October 1989 for a tidal coefficient of 75 (a tidal coefficient is a number that is used to calculate the water level at high and low water with respect to the lowest water level during an equinoctial spring tide) by comparing the real velocities with the calculated ones and by studying the water behaviour along the northern border (compared with data from tidal tables). The model does not include the water contribution from the Odiel river stream flow nor the marsh area (located at the west shore of the river) flooding, since it occurs only in the case of extreme high tides. The model has been developed to study low and medium tides. It represents the most general case since during a normal month there are not more than six or seven tides with a tidal coefficient higher than 90 over a total number of 60 tidal cycles.

The boundary condition used in the hydrodynamic model involves

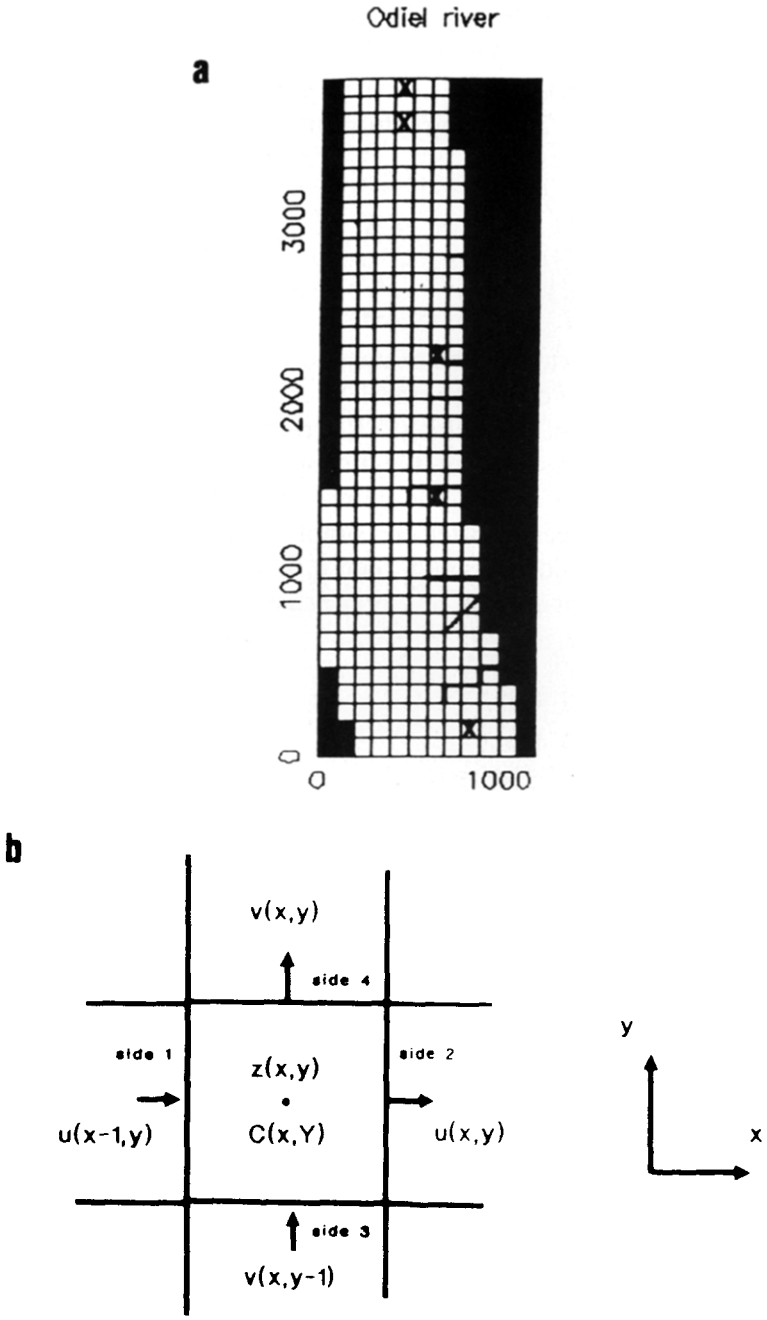

Fig. 2. (a) The grid used in the numerical model; white cells represent water and the black ones land. The crosses (×) are the points at which samples were collected to measure ^{226}Ra concentrations. The grid lengths are $\Delta x = \Delta y = 100$ m. (b) The centring scheme used to solve equations.

making the water displacement z in row $y = 38$ (north boundary) equal to that of row $y = 37$. This is known as a radiation condition.

To solve the dispersion equation, the following finite difference technique was used (see Fig. 2(b) for graphical illustrations):

$$\begin{aligned}\Delta x\Delta y[H^*(x,y)C^*(x,y) - H(x,y)C(x,y)] &= \Delta y H_1 u(x-1,y)\\ &[n_1 C(x-1,y) + (1-n_1)C(x,y)]\Delta t\\ &+ n_1'\Delta y K_u(x-1,y)H_1\frac{C(x-1,y)-C(x,y)}{\Delta x}\Delta t + \ldots\end{aligned} \tag{9}$$

where * indicates the value to be calculated at the new time step and H_1 is the water depth in the centre of side 1 of compartment (x, y). The difference in the content of particles (^{226}Ra radionuclides) in compartment (x, y) is written as the sum of the transport (advective + diffusive) of particles through each side of the compartment. The transport through sides 2, 3 and 4 has been omitted for simplification. n_1 and n_1' are used in the following way: if side 1 is land, then n_1' is zero so as to avoid diffusive transport through that side; in any other case $n_1' = 1$. On the other hand, we have:

$$n_1 = 1 \text{ if } u(x-1,y) > 0$$
$$n_1 = 0 \text{ if } u(x-1,y) < 0$$

so the advective flux of particles is always in the same direction as the velocity.

In the dispersion model, boundary conditions must be specified in both the southern and northern borders. In the northern border, concentrations in row $y = 38$ were made equal to concentrations in row $y = 37$. This condition is equivalent to that used in the hydrodynamic model. In the southern border, the boundary conditions are the following:

$$C_1 = 0{\cdot}98C_2 \text{ for all } v(x,1) < 0$$
$$C_1 = 1{\cdot}02C_2 \text{ for all } v(x,1) > 0$$

So, when water is leaving the grid, we simulate the decay of activity concentrations. On the other hand, when water enters the grid, the multiplicative factor 1·02 produces an increase of concentrations because of the input of contaminated water.

The dispersion model for ^{226}Ra in the Odiel river was tested by balancing at each time step the number of particles in the system. Thus, for each time step the particle number inside the grid and those which leave or enter the southern and northern borders are counted. The total number of particles counted in such a manner should be equal to the particles which

entered the grid from the source. In a simulation over six tidal cycles with a time step of 6 s, the difference in the number of particles is always less than 1%. This can be confidently attributed to the inherent precision of calculations.

4 RESULTS: WATER CIRCULATION AND ^{226}Ra DISPERSION

Some different runs have been performed in order to calibrate the hydrodynamic model against field data and literature information. Following this process, the final value of K was selected as $K = 0{\cdot}0025$.

In Fig. 3 we can see a map of velocities and elevations in the grid when the water level is increasing and decreasing. As is shown in Fig. 3, the water moves along the y-axis. The x-component of the velocity is very small, so there is no important transversal water movement. Figure 4 shows the time evolution of the elevation and velocity of water in two

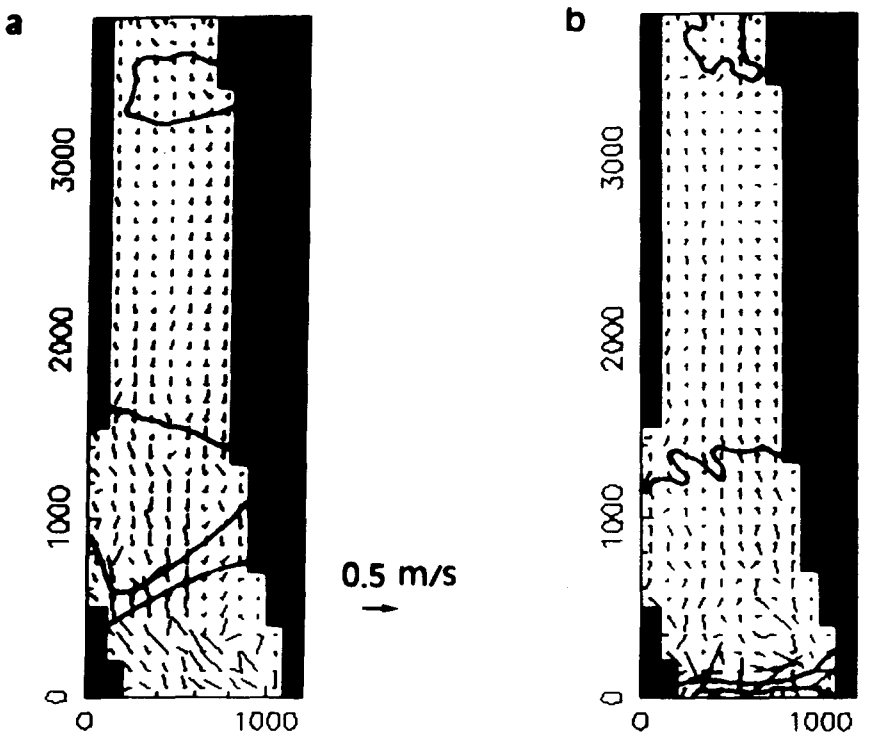

Fig. 3. Velocities and elevation maps: (a) when the water level is increasing (the step between continuous lines is 3 mm, starting with 0·041 m in the southern border); (b) when the water level is decreasing (the step is 5 mm starting with 0·969 m).

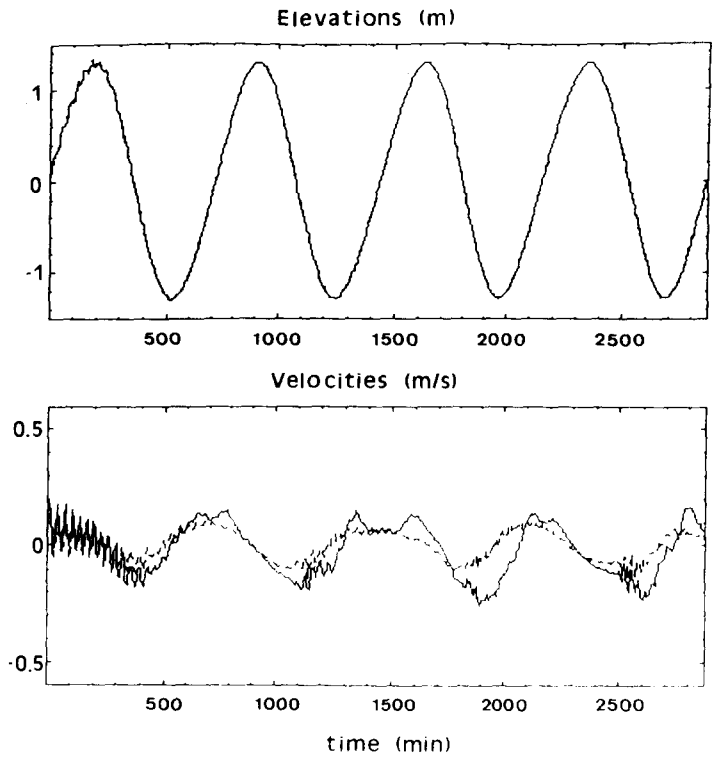

Fig. 4. Time evolution of (a) water elevations and (b) velocities along the y-axis in a compartment near the southern border (continuous line) and in a compartment in the middle of the grid (dotted line). The time is expressed in minutes, elevations in metres and velocities in metres per second. The differences in elevations are a few centimetres, so elevations for both compartments are represented by the same curve.

compartments of the model during several tidal cycles. Calculated velocities are similar but not equal to those experimentally obtained. Indeed, maximum and minimum water velocities in the southern border are 0·48 and $-0{\cdot}66\,\mathrm{ms}^{-1}$, respectively, while the calculated values are 0·38 and $-0{\cdot}51\,\mathrm{ms}^{-1}$. However, we must take into account that we have calculated depth averaged velocities (u) and the experimental data are surface velocities (u_s). The relationship between them (Pugh, 1987) is:

$$u = \alpha u_s$$

where the experimentally measured values of α range from 0·83 to 0·88. Thus, by taking $\alpha = 0{\cdot}84$, the calculated surface velocities are 0·45 and $-0{\cdot}61\,\mathrm{ms}^{-1}$, which are very close to the experimental results. As can be seen in Fig. 4, water elevations are practically the same all along the grid, which corresponds to the real situation since, as seen in tidal tables, the

differences in water elevations are a few centimetres along the grid length. So, the hydrodynamic model results can be considered representative of the site in a situation of medium tides.

Once the hydrodynamic model has been calibrated, the dispersion equation is included.

In Fig. 2(a) (grid covering the Odiel river), sampling stations are marked with an X. The sample in compartment (7,23) was collected in the outlet of one of the fertilizer factories and a peak of activity was measured there. Such a compartment will act as the source of activity to the Odiel River.

After some runs, it was observed that no important changes in activity concentrations occurred when the parameters β_1 and β_2 were slightly varied (see Section 5). So, the authors took $\beta_1 = \beta_2 = 1000$ s, as is given in the literature (Prandle, 1984).

As an example, we can see in Fig. 5 the time evolution of an instantaneous discharge of activity at compartment (7,23) during a tidal cycle. Four photographs were taken, with an interval of 3 h between each. The contamination pulse follows the water movement upstream and downstream through the effects of tidal oscillations and diffusive transport. The major part of the activity always remains in the grid, which means that it was appropriately chosen.

As mentioned in Section 1, samples were collected during high and low water for each sampling campaign. The results for each campaign will be discussed separately.

During the campaign of 1990, the high water samples were collected at about 14:00 h of 19 July 1990, while the low water samples were collected at about 08:30 h of 20 July 1990. In the first case, the wind blew from the north-west with a velocity of 4·1 ms^{-1} and the atmospheric pressure was 1010·8 HPa. In the second case the wind was calm and atmospheric pressure was 1012·9 HPa. The tidal coefficients were 62 in the first case and 68 in the second case. Thus, the real situation was under conditions for which the hydrodynamical model has been calibrated.

In Fig. 6 results corresponding to the year 1990 are shown. The points represent experimental results and the continuous line the calculated activity concentrations. To plot the calculated activities a longitudinal section of the river was studied according to the locations where samples were collected. To reproduce experimental data a simulation over six tidal cycles was performed. Activity input began in cycle no. 3 with an input rate of $2{\cdot}13 \times 10^5$ Bq per time step. This input lasted 3·3h. A second activity input began in cycle no. 6 and lasted 9h; the input rate was now $1{\cdot}35 \times 10^4$ Bq per time step. High water activity concentrations were obtained from cycle no. 5, while the low water ones were from cycle no. 6. Thus we reproduce the sampling campaign conditions. Indeed, high and

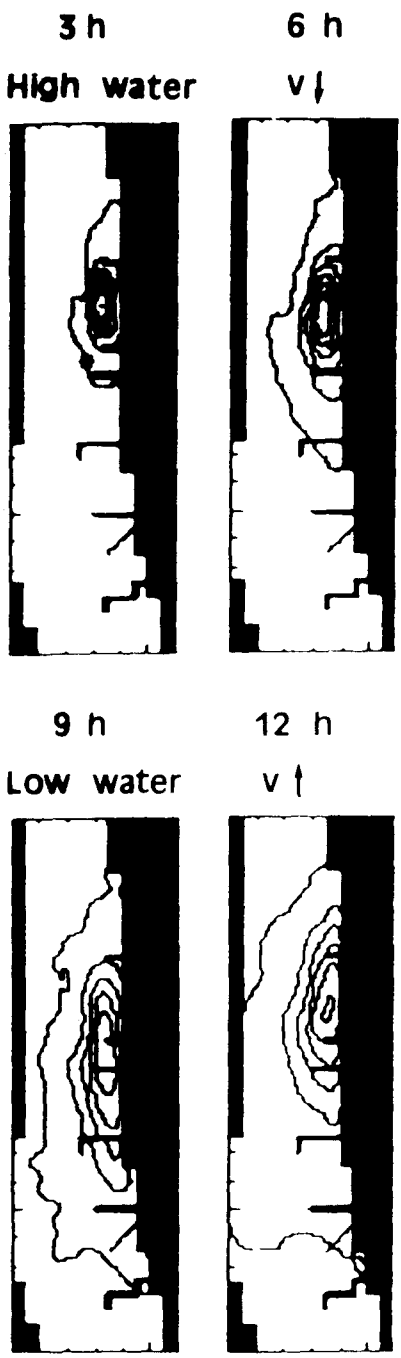

Fig. 5. Time evolution of an instantaneous activity input in the compartment marked with an asterisk. The input was performed at the beginning of a tidal cycle, when water is at the mean level, and the time interval between each map is 3 h.

low water samples were collected with a time difference of 18 h between them.

The initial conditions used in the dispersion model consisted of taking $C = 0$ in the grid, but in the Odiel River there is an important background of ^{226}Ra activity. The first activity input is higher than the second one because it is used to create that background. Thus, before the second activity input we must allow the first one to be distributed along the river, so two tidal cycles are elapsed between them. A sensitivity test has been performed in order to demonstrate that this method of creating a background is not influential on the results. This will be discussed in the next section.

The input rates were changed until the model reproduced the experimental data. As can be seen in Fig. 6, the agreement is rather good with the exception of the activity peak. The real peak is more intense than the calculated one. This is due to the fact that this sample was collected just in the effluent of one of the fertilizer factories. Thus, the activity should be very high. On the other hand, we are assuming instantaneous homogenization in each compartment. Consequently, the calculated activity concentration in the source point must be lower than the real one.

The activity concentration differences between both tides are clear from Fig. 6. They are due not only to the input of non-contaminated water from the sea, but also to a non-constant activity input from the source.

The magnitude of the input rate has been evaluated in order to show it is comparable to that of other fertilizer factories. An average input rate of 3036 Bq s^{-1} was used. This number seems too high. However, it corresponds to an input of $9{\cdot}5 \times 10^{10}$ Bq/year and it has been estimated (Van der Heijde *et al.*, 1988) that $1{\cdot}6 \times 10^{12}$ Bq of ^{226}Ra are annually discharged in the Nieuwe Waterweg (Netherlands) from fertilizer processing.

The high water samples corresponding to the 1991 sampling campaign were collected at about 13:00 h of 5 March 1991 with an atmosphere pressure of 1007 HPa and a north-west wind speed of 6 ms^{-1}. The low water samples were collected one week later, at about 12:00 h of 12 March 1991. The atmospheric pressure was 1006 HPa and wind speed (north-west) was 7 ms^{-1}.

1991 results are presented in Fig. 7. The samples from high and low water were collected with a period of a week between them due to technical problems. So the non-constant input rate from the source is now very important. To ensure that the concentrations in high and low water are not related, several tidal cycles were introduced between them during the simulation. For both low and high water activity concentrations, activity inputs were done in the same way: short discharges during high water were used and the input rates were $1{\cdot}52 \times 10^7$ and $6{\cdot}07 \times 10^6$ Bq per time step, respectively. Activity concentrations were obtained three tidal cycles after the discharge.

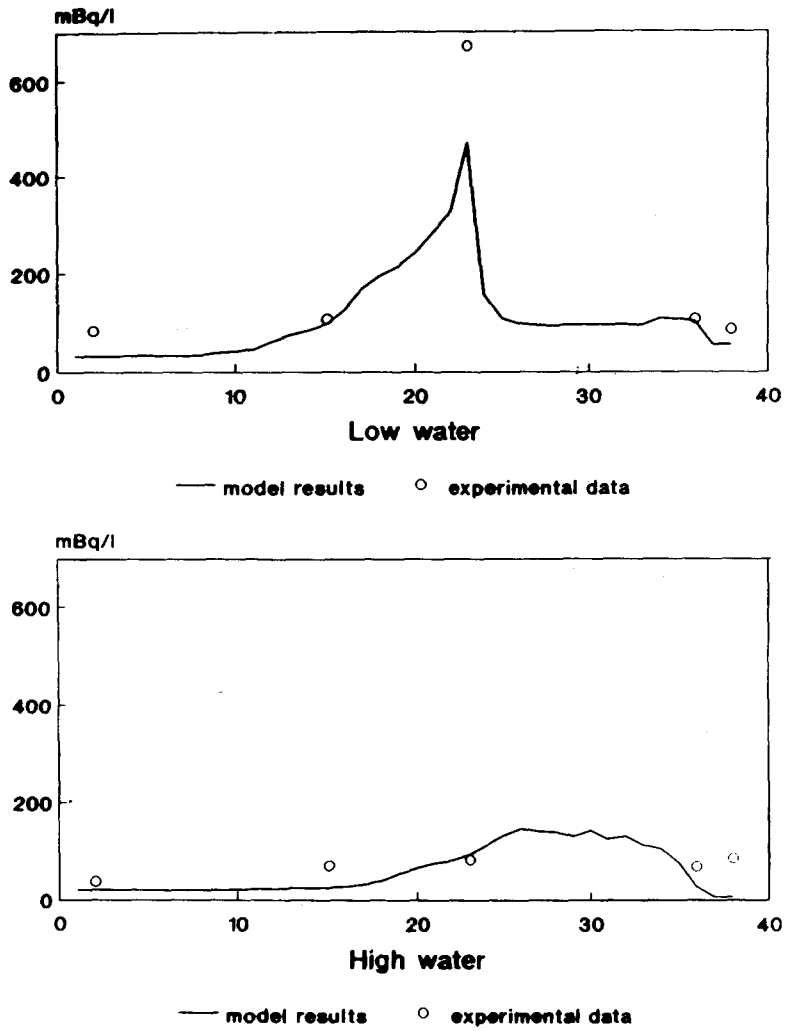

Fig. 6. Model results for the 1990 sampling campaign; experimental results are also shown (white circles). The x-axis corresponds to the position in the grid (see Fig. 2).

As can be seen in Fig. 7, the ^{226}Ra behaviour during the 1991 sampling campaign is well reproduced with the selected source.

It is interesting to note that the weather conditions have not been included in the hydrodynamical model. In spite of that, both the 1990 (dry season) and 1991 (wet season) experimental results are adequately reproduced. The weather conditions obviously affect the stream flow in the Odiel river. In fact, during 1990 the stream flow was around $4\,m^3\,s^{-1}$ while in 1991 it ranges from 25 to $50\,m^3\,s^{-1}$. Therefore, the model seems to be valid for most of the weather conditions and one can conclude that the

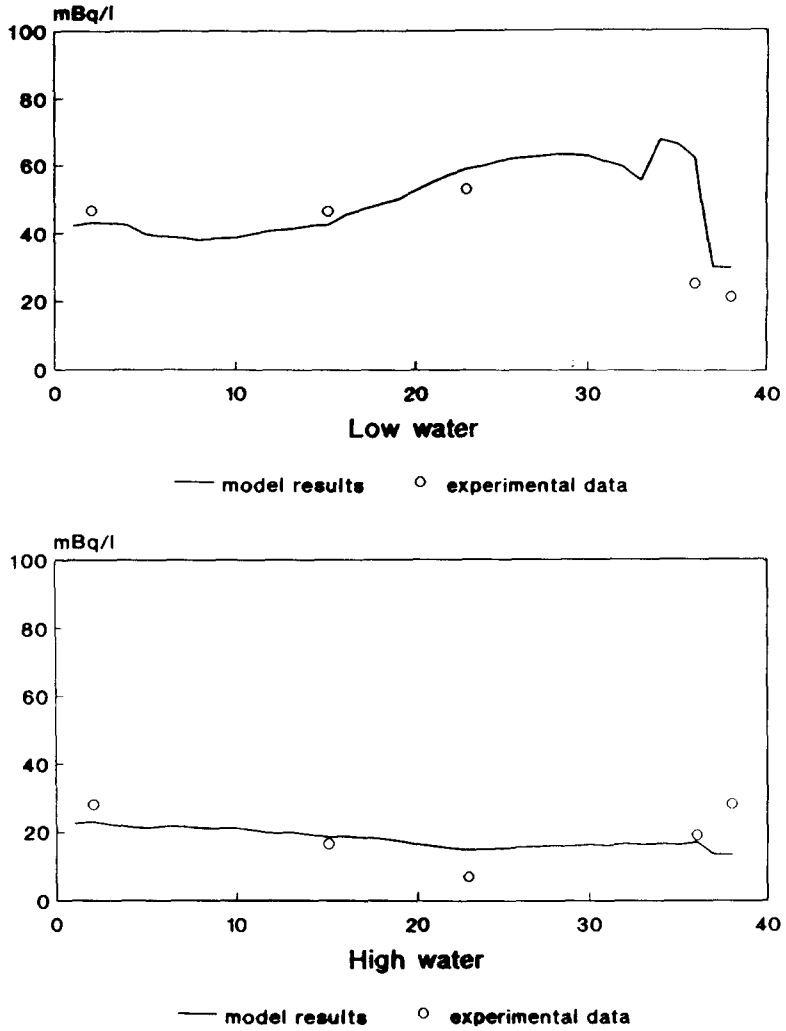

Fig. 7. As for Fig. 6 but for the 1991 sampling campaign.

^{226}Ra activity concentrations along the Odiel River are essentially influenced by the source term. It is probable that in the case of heavy rainfalls, when stream flows can reach very high values, weather conditions can be significant and this model should not be used.

5 SENSITIVITY TESTS

Some sensitivity tests have been performed in order to study the model response to changes in source term, boundary conditions and diffusion coefficients. These tests were done only for the 1990 simulation.

First, the authors studied to what extent variation of the number of particles (Bq) introduced in the river per time step affects the activity concentrations. This is shown in Fig. 8. It can be seen that by increasing the input rates by a factor of two, concentrations which are far too high occur, especially during low water. On the other hand, if the input rates are halved, activity concentrations are too low. Nevertheless, the shape of the distributions is the same in all cases.

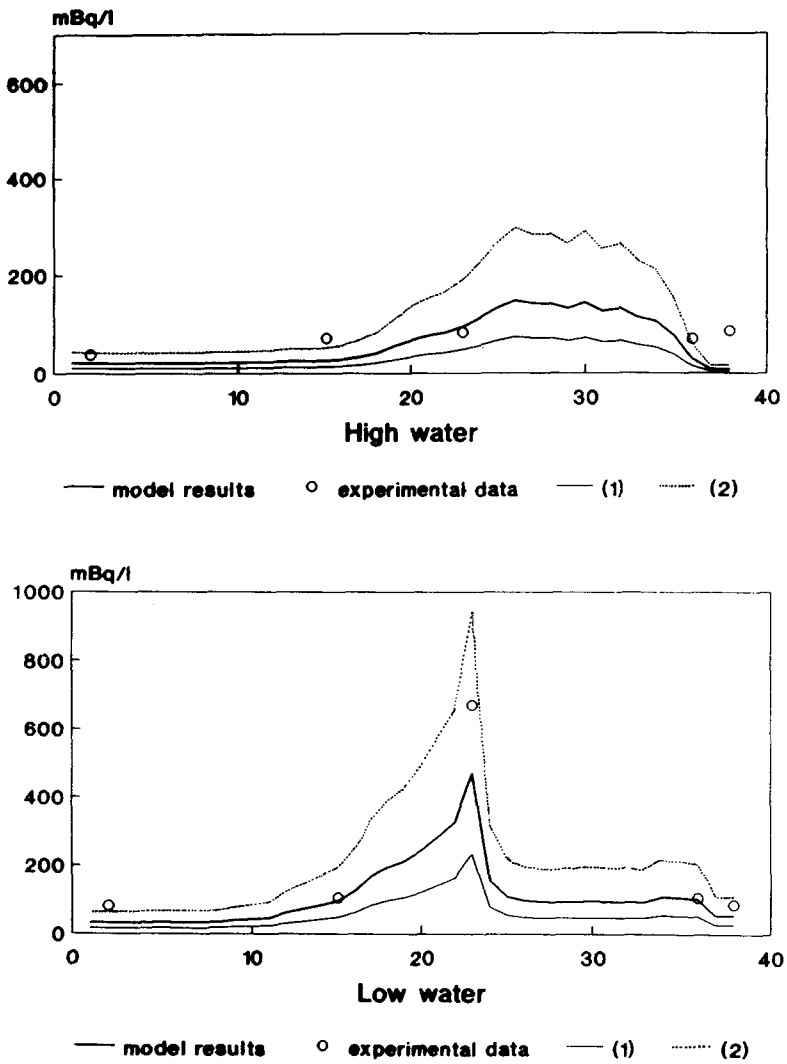

Fig. 8. Sensitivity test to study the model response to a different input rate: (1) results with double input rates and (2) results when they are half the ones used in this study (see text).

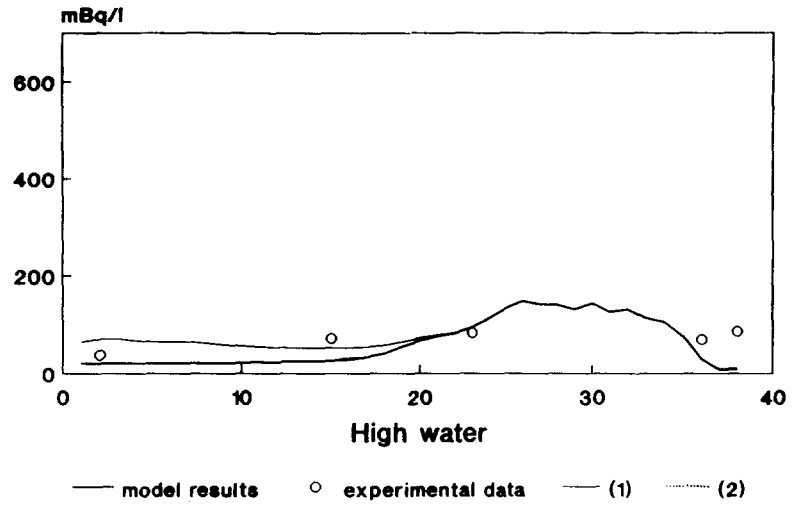

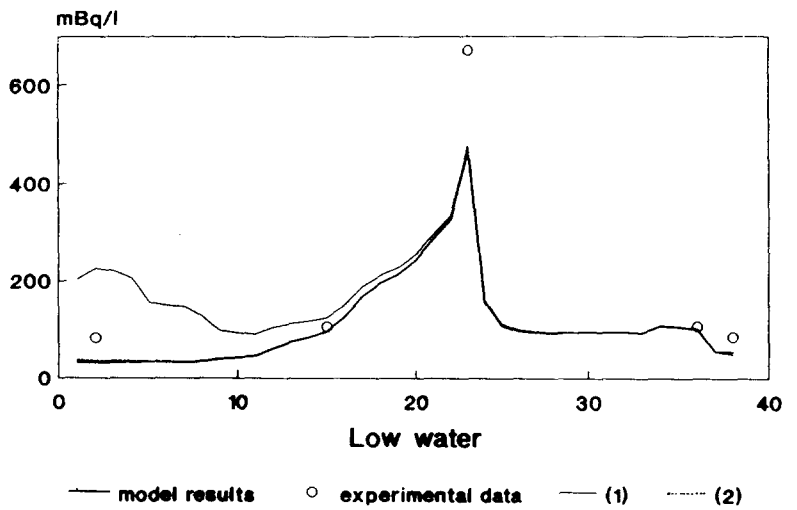

Fig. 9. Model response to variations in boundary conditions in the southern border. (1): $C_1 = 1{\cdot}1C_2$ if $v(y = 1) > 0$ and $C_1 = 0{\cdot}9C_2$ if $v(y = 1) < 0$. (2): $C_1 = C_2$.

The response to changes in boundary conditions is show in Fig. 9. As can be seen, concentrations upstream are not affected by downstream boundary conditions. If we make the concentrations in row 1 proportional to 1·1 or 0·9 (depending on water velocity direction) times the concentrations in row $y = 2$, the calculated concentrations are higher than the measured ones. Thus, these conditions have not been used. In the other two cases, results are

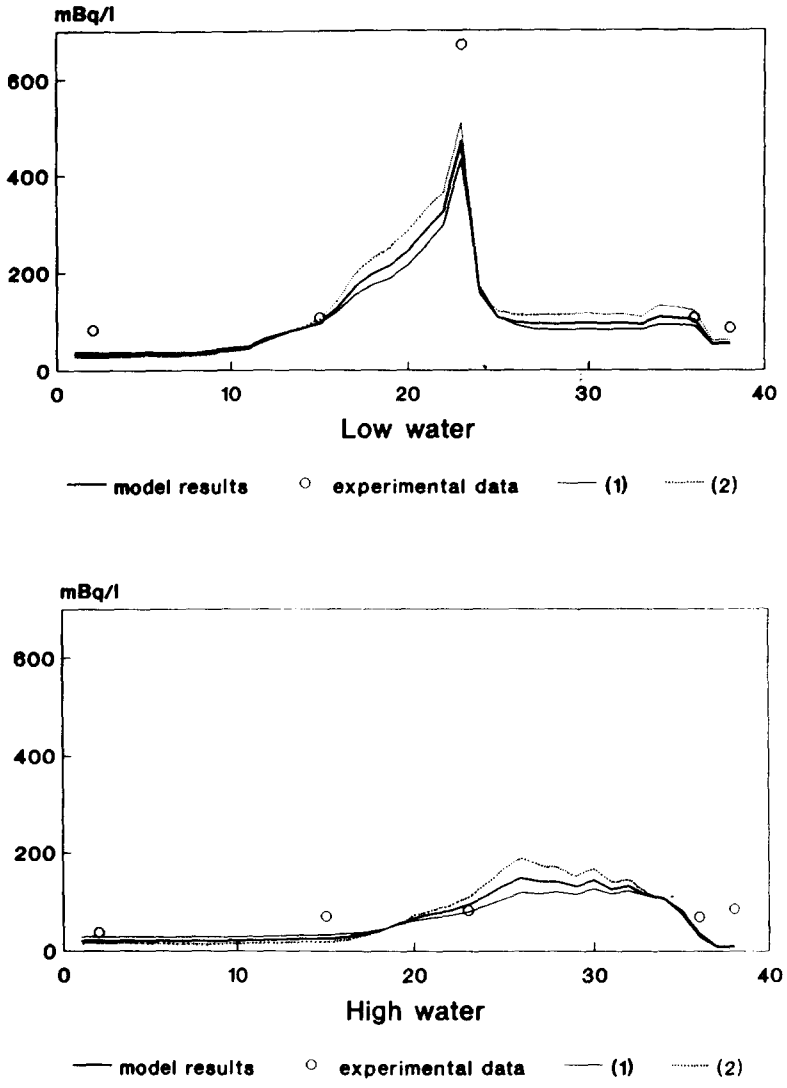

Fig. 10. Responses to changes in β_1 and β_2. (1): $\beta_1 = 1100$ and $\beta_2 = 2000$ s. (2): $\beta_1 = \beta_2 = 500$ s.

very similar. The authors have chosen 1·02 and 0·98 as proportional factors instead of 1 because the 1991 results are better reproduced.

In Fig. 10 we can see that there is no clear difference in the results if changes in diffusion coefficients (β_1 and β_2) are realized. So, the diffusion coefficients used in the model are those found in current literature.

As mentioned in the previous section, a sensitivity test has been carried out by changing the duration of the first activity input (used to create the

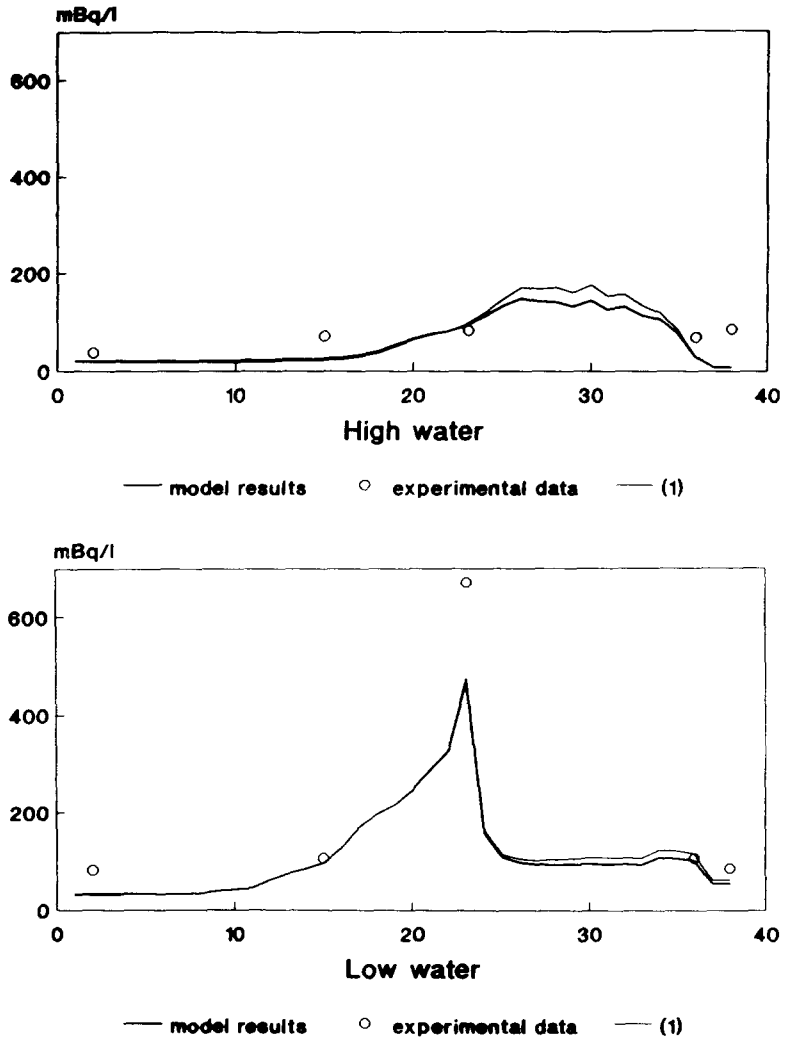

Fig. 11. Model results when the activity background was created in 3·3 h and when it was in 9 h (1).

^{226}Ra background): the same activity is discharged during 9 h instead of 3·3 h. The result can be seen in Fig. 11: there are no important changes in the activity profiles.

6 CONCLUSIONS

A numerical model for the tide and wind induced dispersion of a conservative substance has been developed. It has been applied to ^{226}Ra disper-

sion in an estuarine system of the south-west of Spain affected by fertilizer production (Odiel River). The model is based on the resolution of the hydrodynamic equations considering advection and diffusion as the transport mechanisms.

The hydrodynamic model has been calibrated against literature and field data and it is useful under most conditions: medium and low tides without torrential rains. The selected grid size has shown to be acceptable to study the dispersion of the ^{226}Ra released by the fertilizer plant.

The model has been shown to be able to reproduce experimental results in ^{226}Ra concentrations and has allowed the authors to investigate the magnitude of the activity input from the fertilizer plant, which was not previously known. It has been found that the magnitude of this input is comparable to that from a similar European fertilizer plant. The model has shown that activity concentration differences are mainly due to different source terms.

ACKNOWLEDGEMENT

This work was partially supported by ENRESA and the Spanish DGICYT (contract no. PB89-0621).

REFERENCES

Elsinger, R. J. & Moore, W. S. (1980). ^{226}Ra behavior in Pee Dee river–Winyah bay. *Planet. Sci. Letters*, **48,** 239–49.

Heijde, H. B. van, Klijn, P. J. & Passchier, W. F. (1988). Radiological impacts of the disposal of phosphogypsum. *Radiat. Protect. Dosim.*, **24,** 419–23.

Kobal, I., Brajnik, D., Kaluza, F. & Vengust, M. (1990). Radionuclides in effluent from coal mines, a coal fired power plant, and a phosphate processing plant in Zasavje, Slovenia (Yugoslavia). *Health Physics*, **58,** 81–5.

Koster, H. W., Marwitz, P. A., Berger, J. W., Weers, A. W. van, Hagel, P. & Nieuwenhuize, J. (1991). ^{210}Po, ^{210}Pb, ^{226}Ra in aquatic ecosystems and polders, anthropogenic sources, distribution and enhanced radiation doses in the Netherlands. In Proc. 5th: Int. Symp. on the Natural Radiation Environment, Saltzburg.

Paul, A. C., Londhe, V. S. & Pillai, K. C. (1980). Radium-228 and Radium-226 levels in a river environment and its modification by human activities. *Natural Radiat. Environ.*, **3**(2), 1633–54.

Periáñez, R. & García-León, M. (1993). Ra-isotopes around a phosphate fertilizer complex in an estuarine system at the southwest of Spain. *J. Radioanal. Nucl. Chem.*, **172,** 71–9.

Periáñez, R., García-León, M. & Abril, J. M. (1994). Ra-isotopes in suspended matter in an estuarine system at the southwest of Spain. *J. Radional. Nucl. Chem.*

Prandle, D. (1974). A numerical model of the southern North Sea and River Thames. Institute of Oceanographic Sciences, Report 4, IOS/R/4.

Prandle, D. (1984). A modelling study of the mixing of ^{137}Cs in the seas of the european continental shelf. *Phil. Trans. R. Soc. Lond. A*, **310**, 407–36.

Puerto Autónomo de Huelva (1989). Estudio de corrientes en la ría de Huelva, seguda fase. Private technical report produced by INTECSA (in Spanish).

Pugh, D. T. (1987). *Tides, Surges and Mean Sea-Level.* John Wiley & Sons, Chichester.